Imaging single synaptic vesicles undergoing repeated fusion events: kissing, running, and kissing again

A.M. Aravanis [a,b], J.L. Pyle [a], N.C. Harata [a], R.W. Tsien [a,*]

[a] *Department of Molecular and Cellular Physiology, B105 Beckman Center, Stanford University School of Medicine, Stanford, CA 94305, USA*
[b] *Department of Electrical Engineering, Stanford University, Stanford, CA 94305, USA*

Abstract

At synapses of the mammalian central nervous system, release of neurotransmitter occurs at rates transiently as high as 100 Hz, putting extreme demands on nerve terminals with only tens of functional vesicles at their disposal. Thus, the presynaptic vesicle cycle is particularly critical to maintain neurotransmission. To understand vesicle cycling at the most fundamental level, we studied single vesicles undergoing exo/endocytosis and tracked the fate of newly retrieved vesicles. This was accomplished by minimally stimulating boutons in the presence of the membrane-fluorescent styryl dye FM1-43, then selecting for terminals that contained only one dye-filled vesicle. We then observed the kinetics of dye release during single action potential stimulation. We found that most vesicles lost only a portion of their total dye during a single fusion event, but were able to fuse again soon thereafter. We interpret this as direct evidence of "kiss-and-run" followed by rapid reuse. Other interpretations such as "partial loading" and "endosomal splitting" were largely excluded on the basis of multiple lines of evidence. Our data placed an upper bound of <1.4 s on the lifetime of the kiss-and-run fusion event, based on the assumption that aqueous departitioning is rate limiting. The repeated use of individual vesicles held over a range of stimulus frequencies up to 30 Hz and was associated with neurotransmitter release. A small percentage of fusion events did release a whole vesicle's worth of dye in one action potential, consistent with a classical picture of exocytosis as fusion followed by complete collapse or at least very slow retrieval.
© 2003 Elsevier Ltd. All rights reserved.

1. Introduction

Neuronal communication in the mammalian brain relies in large part on the release of neurotransmitter from synaptic vesicles at nerve terminals averaging ~1 µm in diameter (Harris and Sultan, 1995; Schikorski and Stevens, 1997; Harata et al., 2001b). Unlike the best characterized neurosecretory preparations, the presynaptic terminals of small central synapses typically contain less than 30 functional vesicles at any given time (Murthy and Stevens, 1999; Harata et al., 2001a), and it is likely that a terminal under continuous operation has even less (Dobrunz and Stevens, 1997). A single synapse in the mammalian hippocampus can be called upon to

release 4000 vesicles an hour, a demand that would quickly overwhelm a presynaptic terminal without a local mechanism to replenish synaptic vesicles (Sudhof, 1995, 2000; Harata et al., 2001a). The way that these terminals make use of their limited vesicle pools during continual operation is an important factor governing the capacity for information transfer across synapses in the central nervous system (Dobrunz and Stevens, 1997; Harata et al., 2001a).

In the "classical model" of the synaptic vesicle cycle, first described at the frog neuromuscular junction (Heuser, 1989; Sudhof, 1995), vesicle fusion results in the complete collapse of a vesicle into the plasma membrane, and consequently, a requirement that new vesicles be created directly from the plasma membrane. This model is supported by studies in secretory systems that maintain their vesicle pool by clathrin and endosome-dependent endocytosis of secretory vesicles (Heuser and Reese, 1973; Marsh and Mcmahon, 1999). A mechanism

* Corresponding author. Tel.: +1-650-725-7557; fax: +1-650-725-8021.

E-mail address: rwtsien@stanford.edu (R.W. Tsien).

of de novo synthesis is critical for a depleted presynaptic terminal to replenish itself following exhaustive stimulation, and was among the first features of the vesicle cycle to be described in small central synapses (Liu and Tsien, 1995; Ryan et al., 1996). The classical model has been contrasted with the "kiss-and-run" model of vesicle cycling, which allows for fusion without complete loss of vesicle identity (Ceccarelli et al., 1973; Palfrey and Artalejo, 1998; Sudhof, 2000; Klyachko and Jackson, 2002).

Specialized nerve terminals such as the neuromuscular junction, the retinal bipolar synapse, and the Calyx of Held have allowed detailed measurements of neurotransmitter release, lipid marker trafficking, and capacitance changes (Ribchester et al., 1994; Neves and Lagnado, 1999; Schneggenburger et al., 1999; Zenisek et al., 2000). Unfortunately, studies in these preparations have led to conflicting predictions on the behavior of a single vesicle within a central synapse. The methods available to measure the behavior of single vesicles in other preparations are limited when applied to the small central terminal. The tiny surface area of most central terminals prevents the use of capacitance measurements that are feasible at larger terminals (Klyachko and Jackson, 2002; Sun et al., 2002). Most terminals in the mammalian brain do not contain catecholamine neurotransmitters suitable for detection by amperometry (cf. Kim et al., 2000). Single synaptic vesicles can be visualized in the large presynaptic nerve terminal of goldfish bipolar neurons by use of total internal reflection (TIR) imaging (Zenisek et al., 2000; Zenisek et al., 2002); however, the complex three-dimensional structure of an intact, central synapse prevents the direct contact between fusion site and glass substrate that would be needed for TIR.

Previous studies have approached the function of small central terminals through direct measurements of neurotransmitter release from a large number of nerve endings, or by monitoring the release of styryl dyes from a large number of synaptic vesicles (Stevens and Tsujimoto, 1995; Ryan, 1996; Klingauf et al., 1998; Murthy and Stevens, 1999; Stevens and Wesseling, 1999; Pyle et al., 2000; Stevens and Williams, 2000; Sara et al., 2002). Recent evidence indicates that vesicles are able to release neurotransmitters in a manner that does not require the complete collapse of the vesicle (Klingauf et al., 1998; Pyle et al., 2000; Stevens and Williams, 2000; Sara et al., 2002). Based upon the release of multiple FM dyes (Klingauf et al., 1998) and combined measurements of neurotransmitter and FM2-10 release (Pyle et al., 2000; Sara et al., 2002) we predicted that vesicles in small central synapses should be able to fuse multiple times in quick succession. This mechanism would permit a single vesicle to support multiple neurotransmission events. Here, we provide a detailed description of a study of the vesicle cycle at its most fundamental level—

through direct monitoring of the behavior of a single synaptic vesicle as it undergoes fusion and retrieval, often in repeated cycles. We relate our findings to other approaches to study vesicle dynamics at the level of unitary events (Zenisek et al., 2002; Gandhi and Stevens, 2003).

Some of this work was presented previously in an abbreviated format (Aravanis et al., 2003).

2. Methods

2.1. Cell cultures

CA3–CA1 hippocampal neurons of P0–P1-day-old Sprague–Dawley rats were prepared in sparse culture according to previous protocols (Malgaroli and Tsien, 1992; Liu and Tsien, 1995) with minor modifications, and used for imaging after 12–18 days in vitro. In order to measure the fluorescence of hundreds of molecules of FM1-43 over background fluorescence, we enforced the most exacting standards for our biologic samples. We performed more than 50 independent cultures, generating more than 600 individual coverslips of primary CA1–CA3 hippocampal neurons. Approximately, half of these batches were excluded from further experiments by their bright-field appearance alone. Our rigorous standards for selection at this level included the overall density of neurons, the ratio of neurons to glia, the quality and number of dendritic processes, and the formation of numerous and healthy appearing processes on bare glass. We screened the remaining cultures by test staining and de-staining selected coverslips with a greater than minimal loading of FM1-43, a procedure designed to evaluate the optical properties of the stained boutons and the regions around them. Biological debris, dead cells (neurons or glia), and even small fragments of non-biological matter stained brightly with FM-143 during brief exposures to the dye. The presence of any of the non-specific FM1-43 fluorescence made coverslips unusable for further experiments. Of the approximately 30 independent culture batches evaluated in this manner, seven were determined to have a potentially useful subset of coverslips. The optical requirements for minimal-staining experiments were even more exacting: out of the 84 coverslips selected from the seven independent cultures, only 14 coverslips were deemed acceptable for molecular fluorescence measurements. Data presented in this paper where single vesicles were de-stained with 0.125 Hz come from eight of those cover slips; experiments where single vesicles were de-stained with 10 Hz come from the remaining six cover slips. All experiments were performed at 25 °C in physiological solutions containing 2 mM Ca^{2+} and 2 mM Mg^{2+}.

2.2. Dye loading and de-staining

Presynaptic terminals were first labeled by exposure to styryl dye (16 μM FM1-43) during five (Figs. 1 and 6) or ten (Figs. 2 and 3) field stimulus pulses delivered at 10 Hz (platinum bath electrodes delivering 20 mA/1 ms/pulse). This manner of field stimulation elicits physiological vesicle turnover by evoking propagating action potentials in hippocampal neurons (Deisseroth et al., 1996). Application of tetrodotoxin (1 μM) completely eliminated vesicle turnover (data not shown). In a staining protocol designed to allow full staining of individual vesicles, the FM dye was allowed to remain in the extracellular solution for 10 s following stimulation, followed immediately by a wash with a dye-free, modified Tyrode containing 0 Ca^{2+}. All solutions used contained 10 μM CNQX to prevent recurrent activity. De-staining of hippocampal terminals was achieved by additional field stimulation at either 10 Hz (Figs. 1, 6) or 0.125 Hz (Figs. 2–4). Afterwards, terminals were fully de-stained with 600 APs delivered at 10 Hz. Presynaptic terminals were allowed to recover for 3-4 min; then, the entire recycling pool of all synapses was stained by bath application of 16 μM FM1-43 in 45 mM K^+ solution for 90 s (Harata et al., 2001a). Images of the fully stained field were then acquired before and after complete de-staining with three rounds of high K^+ depolarization (60 s each).

2.3. Optical measurements, image analysis, and system calibration

Fluorescence detection of single synaptic vesicles was performed using an inverted epi-fluorescence microscope (TE-200, Nikon), equipped with a high numerical aperture objective (Plan Fluor 40×, 1.3 NA, Nikon). Images were obtained with an intensified CCD camera (XR/Mega-10, Stanford Photonics) operating in gated acquisition mode. For the minimal-staining protocol, the samples were exposed to brief pulses of arc lamp illumination (470/40 nm, Croma Technology Corporation) via an optical switch (Lambda 10-2, Sutter Instrument Corporation). The emission signal was filtered by a 515 nm long-pass optical filter (Croma Technology Corporation). The exposure time per image (15 ms) and intensifier gain (940 V) were chosen to maximize the fluorescence signal while causing no more than 10% photobleaching over 121 images. In the maximal-staining protocol, the intensifier gain and exposure time were lowered to decrease the overall system gain by a factor of 15. This placed the fluorescence of a fully loaded terminal in the dynamic range of the ICCD camera. In all the experiments shown, sequential images were acquired at 0.5 Hz and stimulation was phase-locked to the imaging, the first action potential occurring milliseconds after the 21st image. Fluorescent images were downloaded in
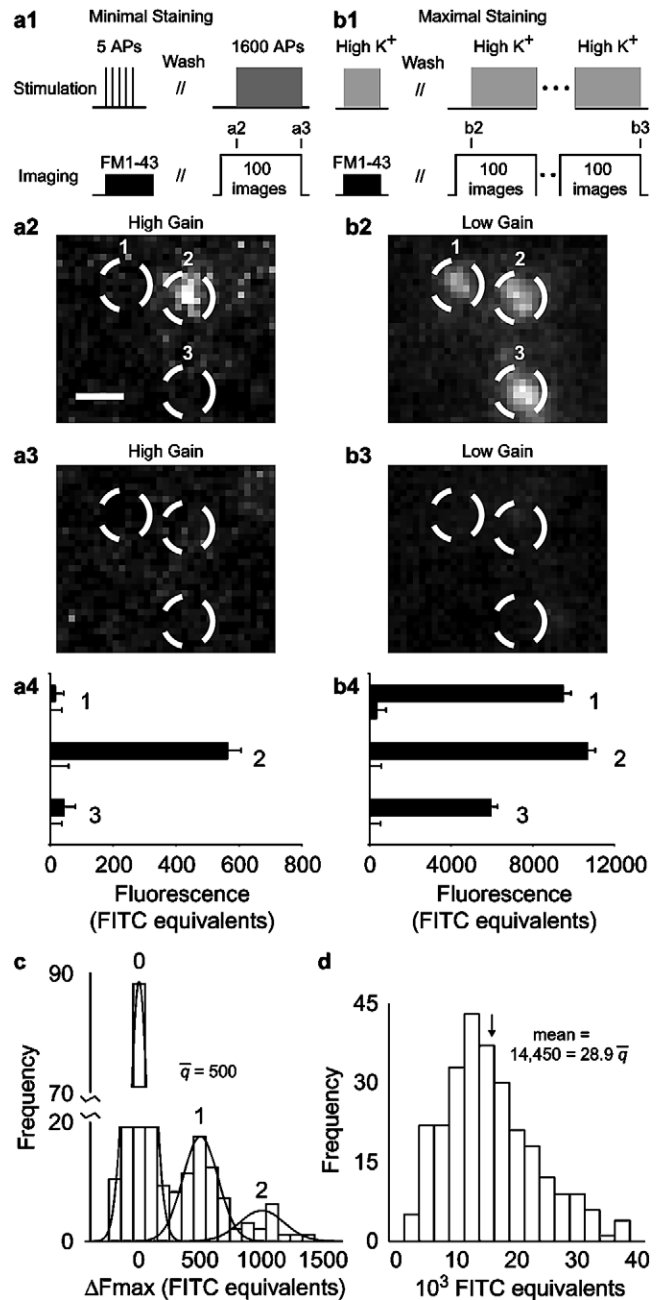

Fig. 1. Quantal staining of FM1-43 at single boutons. (a1) Minimal-staining protocol, field stimulation with 5 stimuli at 10 Hz in 16 μM FM1-43. (a2) Minimally stained region. ROIs 1, 2, and 3 centered on functional presynaptic terminals (see b2). Bouton 2 contained one synaptic vesicle labelled with FM1-43; boutons 1 and 3 contained none. Scale bar, 1 μm. (a3) Same area as a2 after 1600 stimuli (10 Hz). (a4) Fluorescence intensities of each ROI before (top bar) and after stimulation (bottom bars), as in a2 and a3. Error bars, standard deviation of 20 images. (b1) Maximal-staining protocol. (b2) Same area as a2 after maximal-staining. (b3) Same area as b2 after exhaustive de-staining. (b4) Fluorescence intensities of the ROIs before (top bar) and after stimulation (bottom bar), as in b2 and b3. (c) Histogram of the fluorescence change (ΔF_{max}) of minimally stained terminals (*n* = 272). Peaks represent boutons containing zero, one, or two vesicles; quantal spacing ($\bar{q}$), 500 FITC equivalents. (d) Histogram of the estimate number of functional synaptic vesicles in CA1–CA3 terminals. From Aravanis et al. (2003), with permission.
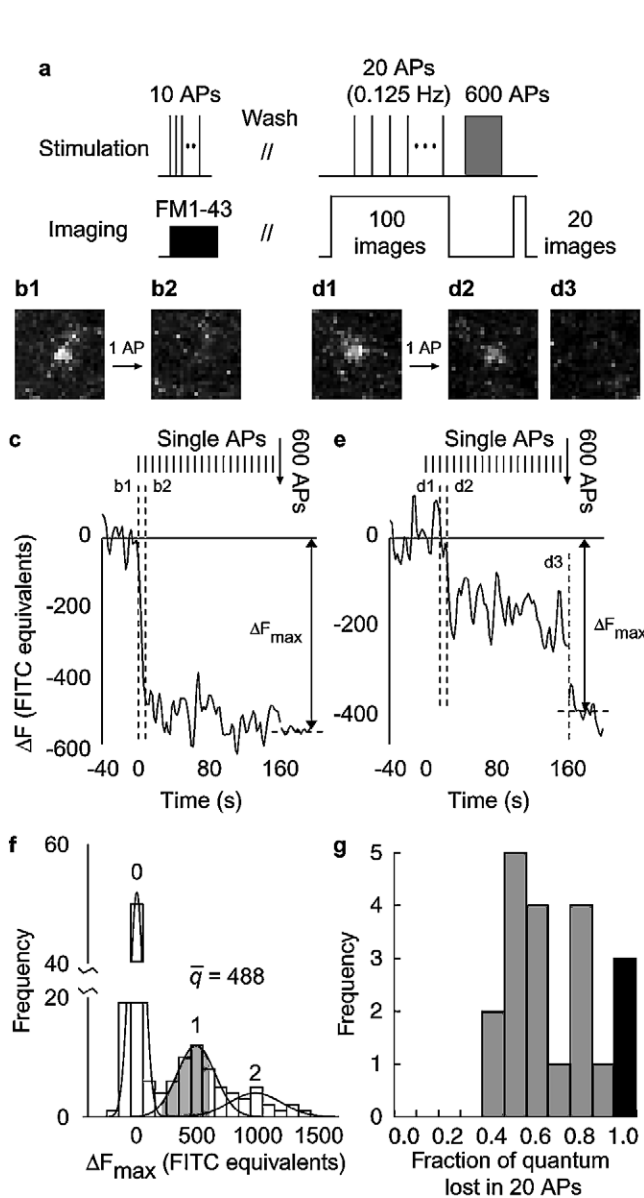
Fig. 2.   Individual fusion events usually result in dye retention. (a) Low-frequency stimulation (4:1 ratio of imaging to APs) allowed the consequences of individual APs to be resolved. (b1,b2) Individual high gain images, taken just before the first and second stimuli. A single vesicle's worth of fluorescence was lost after one AP was elicited. (c) Corresponding fluorescence signal. (d1–d3) Individual high gain images from another experiment, taken just before the 3rd and 4th stimuli and just after 620 stimuli. A fusion event after the 3rd AP was followed by retrieval rapid enough to leave FM1-43 trapped in the vesicle. The remaining fluorescence was retained for 15 APs and then released with 600 APs. (e) Corresponding fluorescence signal. (f) Quantal analysis of fluorescence change before and after exhaustive stimulation ($n = 153$ ROIs). Shaded area in histogram represents single-stained vesicles ($>95\%$ confidence) that were taken for analysis. (g) Most single vesicles (85%) retained a fraction of their original quantum of dye after 20 APs, while 15% lost the full quantum in one AP (dark bar). From Aravanis et al. (2003), with permission.
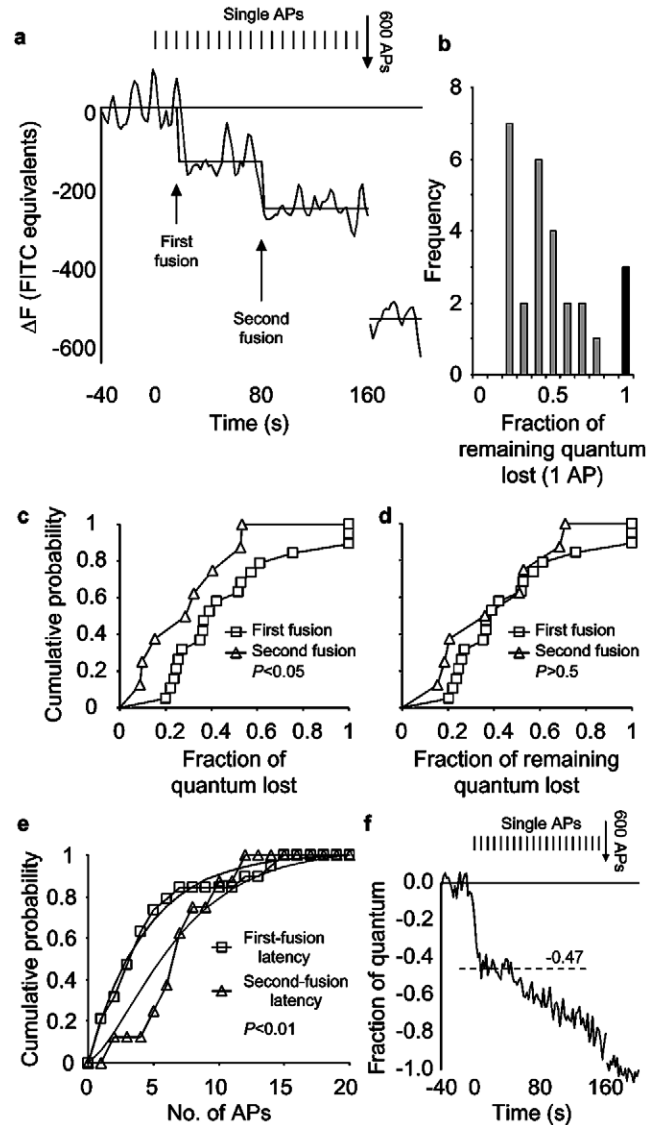

Fig. 3.   Single vesicles can fuse multiple times during 20 APs. (a) A vesicle fused twice (3rd and 11th APs). (b) Histogram of the fraction of the remaining quantum lost in all detectable single fusions. (c) Collected data of fluorescence lost on first ($n = 19$) and second fusions ($n = 8$), shown as cumulative distributions. Mean ΔF on 1st fusions, $0.48q$, on 2nd fusions, $0.30q$ ($P < 0.05$, t-test). (d) Fraction of remaining quantum lost on first and second fusions, given as cumulative distributions. (1st mean = $0.48q$, 2nd mean = $0.42q'$, $P > 0.5$, t-test). (e) Cumulative distributions of first-fusion latency (mean = 4.9 APs, $n = 19$), and second fusion latency (interval between first and second fusions) (mean = 7.1 APs, $n = 8$). First fusion latency was significantly faster than second fusion latency ($P < 0.01$, K–S), indicating that another process delays the second fusion. (f) Average of time-aligned traces ($n = 19$), emphasizing that the first fusion resulted in loss of 47% of the quantum on average, and that second fusion was significantly delayed. From Aravanis et al. (2003), with permission.

a 10 bit digital format (MV-1465, μTech) and observed with MetaFluor (Universal Imaging). Off-line analysis was performed with MATLAB (The MathWorks, Inc.) and custom software. In general, every effort was made to reduce autofluorescence while not compromising
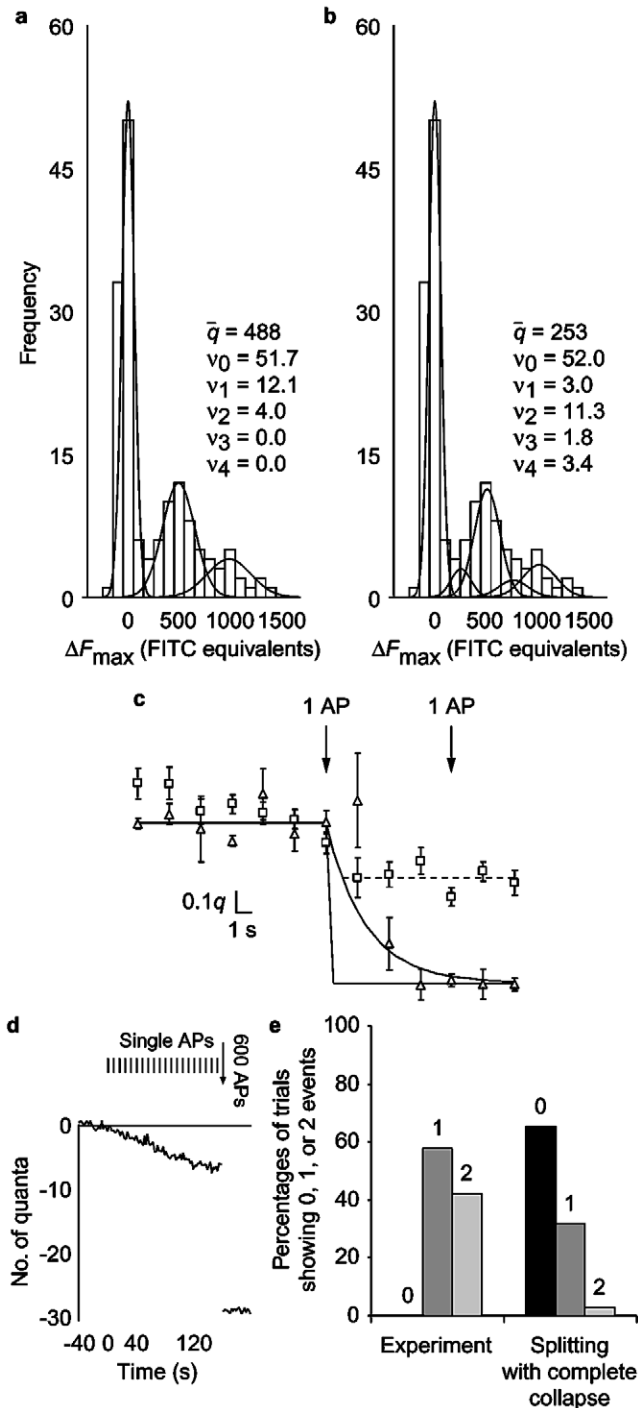
Fig. 4. Consideration of alternative hypotheses for subquantal destaining entailing complete collapse of partially stained vesicles. (a, b) Further exploration of quantal analysis, testing of the possibility of partial loading of vesicles. (a) 10 AP data, fitted with 3 gaussians (for clarity, repeat of Fig. 2f). (b) Same data, fitted with 5 gaussians with the quantal size constrained to be <300 FITC equivalents. Best fit yielded a quantal size of 253 FITC equivalents and did not improve the quality of fit relative to that achieved with 3 gaussians (panel a). Furthermore, the area under the intermediate peaks in b was small compared to that of the main peaks. Hence, the contribution of any partially stained vesicles would have been extremely minor, inconsistent with the observed predominance of subquantal events. (c) Time course of fusions resulting in complete quantal loss (triangles) vs. fusions resulting in partial loss (squares). Traces were normalized to adjust for slight differences in full quantal amplitude, time aligned at the point of stimulation, and then averaged (error bars give standard errors of the mean). The time course of the pooled full release events was consistent with dye release through aqueous departitioning (smooth curve is an exponential with $\tau = 2.5$ s). The time course expected for lateral diffusion is much faster ($\tau \sim 10$ ms, solid gray line). The rapid settling of the partial fusions, within one sample point, was as expected for a fully stained vesicle whose continuity with the external medium was abbreviated before complete loss of dye could occur. Dashed horizontal line is the best fit of the last 4 sample points. The brisk settling argues against the proposal that partially stained vesicles underwent complete collapse. (d, e) Experimental data exclude an explanation of subquantal steps based on a simple model of classical endocytosis in which the fluorescent content of a fully dye-labeled vesicle was internally split into multiple daughter vesicles. (d) Average response ($n = 18$) of maximally stained boutons to 20 stimuli delivered at 0.125 Hz. Individual traces were normalized, averaged, and scaled to the average size of the total recycling pool (Fig. 1d). On average, the equivalent of six fully fluorescent quanta ($6q$) was released after 20 APs. (e) The percentage of trials showing zero (P_0), one (P_1), or two (P_2) fusion events during 20 APs, found empirically and predicted theoretically for the scenario in question. Experiment: actual data, showing no trials completely lacking any fusion event ($P_0 = 0\%$), a majority with one fusion event ($P_1 = 58\%$), and a significant number of double events ($P_2 = 42\%$, see Fig. 5). Splitting with complete collapse: outcome predicted from a scenario in which a single vesicle's worth of FM dye was taken up, but split by endosomal processing into two partially loaded vesicles that distributed themselves randomly within the recycling pool, averaging 29 vesicles in size. Over the course of 20 APs, the two vesicles could then be released independently by complete vesicular collapse. The likelihood that six successful release events would include 0, 1 or 2 partially stained quanta was: $P_0 = (27/29)^6 = 65\%$ $P_1 = \Sigma_{n=0}^{5}(27/29)^n(2/29)(28/29)^{(5-n)} = 32\%$, and $P_2 = 1 - P_0 - P_1 = 3\%$. The predicted values of P_0 and P_2 were in strong disagreement with the experiment, arguing against endosomal splitting followed by random mixing as the explanation for subquantal steps.

escent molecules. We used the psf of our system to select an appropriate region-of-interest (ROI) for imaging single synaptic vesicles. The standard deviation and full-width-half-maximum (FWHM) of the psf were 160 and 370 nm, respectively. To maximize detection of fluorescence from a single synaptic vesicle, we opted to use an ROI with a diameter of 1.09 μm (8 pixels), 6.8 standard deviations of the fitted psf gaussian. This ROI size was also tolerant to variations in z-distance of individual vesicles, because the depth of field of the system, 0.7–1.0 μm (Nikon technical documentation), is approximately the same size as the diameter of hippocampal

other important imaging criteria. ΔF_{max} was the difference between 20-image averages before and after stimulation.

We calibrated the fluorescence intensities detected in our system by imaging 0.87 μm beads coated with 980±15 FITC molecules (custom-made by Bangs Laboratories, Inc). The point-spread function (psf) of our imaging system was determined empirically by repeated imaging of 49 nm beads coated with FM1-43-like fluor-

terminals (<1 μm). We estimate that in the worst case of a vesicle moving from the center to the edge of the depth of focus, a 10% decrease in ROI intensity would occur, small enough not to interfere with our ability to determine the fluorescence of a single vesicle. In fact, changes in vesicle position were uncommon.

2.4. Identification of individual synapses by maximal-staining protocol

All synapses present in our image frames were identified on the conclusion of minimal-staining experiments by the uptake of FM1-43 during a 90-s application of 45 mM K$^+$. We selected synapses for our study by identifying all punctuate regions <1.2 μm in diameter that demonstrated a total release of dye greater than >2500 FITC equivalents (approximately 5 vesicles) during repetitive application of high-K$^+$ solution. A circular ROI (1.09 μm diameter) was centered on the intensity peak of each identified synapse and then referred back to images captured during minimal-staining experiments. The vast majority of synapses identified by high-K$^+$ staining failed to label with any FM1-43 when presented with only 5 or 10 stimuli. The slight amount of photobleaching ($<10\%$) associated with 121 images (15 ms exposure duration) was empirically determined and removed from image time courses by subtraction.

2.5. Selection of single vesicles

The histograms in Figs. 1c and 2f were fit with three gaussians obeying Eq. (1):

$$T(\Delta F) = \sum_{k=0}^{2} v_k e^{-\frac{(\Delta F - kq)^2}{2(\sigma_z^2 + k\sigma_v^2)}} \qquad (1)$$

where T is the total number of events for a given ΔF, v_k is the amplitude of the kth peak, σ_z^2 is the variance of the zero peak and represents measurement error, σ_v^2 is the variance associated with the fluorescence of a single FM1-43 labeled vesicle, and q is the quantal fluorescence. The ΔF values that correspond to one vesicle were estimated by calculating the range of ΔF values that have a $>95\%$ probability of being a member of the $k = 1$ gaussian.

2.6. Analysis of individual fusion events

The timing and magnitude of dye release events were analyzed by first determining the number of dye release events for each single vesicle de-staining trace (stimulated at 0.125 Hz). Fusion events were defined as abrupt and lasting fluorescent decreases $>10\%$ of ΔF_{max}, which represented a true signal change with $>95\%$ confidence. A staircase with the same number of events was then fit to the trace. The timing and magnitude of events

were free parameters determined by best fit, thereby specifying the action potential number and the magnitude of each event. It is possible that some release events occurred that were below the resolution of the measurement; however, the main conclusions of the discrete event analysis were corroborated by analysis of averaged fluorescence traces.

2.7. Photoconversion and electron microscopy

FM dye photoconversion and electron microscopy were performed as before (Harata et al., 2001b).

2.8. Dye loading and de-staining in experiments with combined electrophysiology

Presynaptic terminals were labeled by exposure to styryl dye (8 μM FM1-43 or 400 μM FM2-10) during high-K$^+$ depolarization (modified Tyrode, 45 mM KCl). Dye was allowed to remain in the extracellular solution for 30 s following a staining protocol. Images were taken after 10–15 min washes in dye-free solution. De-staining of hippocampal terminals with hypertonic challenges was achieved by direct perfusion of modified Tyrode (500 mM sucrose added) onto the field of interest, using gravity-driven perfusion or a Picospritzer (General Valve Corporation).

2.9. Electrophysiology

Postsynaptic responses of hippocampal synapses to electrically evoked action potentials were obtained by whole-cell recording using an Axopatch 200B amplifier with Clampex 8.0 software (Axon Instruments). Patch pipettes and stimulating pipettes were pulled from borosilicate glass to a tip diameter corresponding to a resistance of 2–4 MΩ. Internal solution included 135 mM Cs gluconate, 10 mM EGTA, 2 mM MgCl$_2$, 5 mM Mg-ATP, and 10 mM HEPES (pH 7.35). Series resistance and cell capacitance were compensated and the data were filtered at 5 kHz by an 8-pole Bessel filter.

3. Results

3.1. Labelling and imaging single synaptic vesicles

We devised a strategy to label only a small number of vesicles with dye in order to monitor the exocytotic and endocytotic behavior of single vesicles. In the minimal-staining protocol (Fig. 1a1), cultured CA3–CA1 neurons were briefly exposed to FM1-43 while five action potentials (APs) were elicited. The dye was then rapidly washed from the bath, restricting dye exposure to ~10 s. Dye-free solution containing 0 Ca^{2+} continuously perfused the chamber for 15 min to remove extracellular

dye while minimizing the rate of spontaneous exocytosis. The release of dye from synaptic vesicles was then monitored by fluorescence imaging during field stimulation at 10 Hz. A total of 1600 AP stimuli were delivered to release all dye. After a brief rest period, we identified all functional presynaptic boutons in the same field by exposing terminals to high K$^+$-containing solution in the presence of FM1-43 (maximal-staining protocol, Fig. 1b1). Three serial applications of high K$^+$-containing solution released the entire recycling pool of vesicles, de-staining the terminals completely (Harata et al., 2001a).

The images acquired with the maximal-staining protocol clearly identified all the functional synaptic boutons in the fields of view. We used the images of fully loaded terminals to define regions of interest (ROIs) for the retrospective analysis of dye uptake and release resulting from minimal staining. Fig. 1b2, b3 illustrates fluorescence images of an area stained with the maximal-staining protocol, before (b2) and after (b3) stimulation. Three punctate regions corresponding to individual synapses (1, 2, 3) were clearly evident, and were delimited by circular ROIs. The total amount of fluorescence within all three ROIs before and after stimulation was expressed in units of fluorescein isothiocyanate (FITC) molecular equivalents (see Section 2) (Fig. 1b4). Fig. 1a2 shows the same field of view as in b2, but following minimal staining. In this case, only one of the three identified synaptic terminals, bouton 2, was labeled with FM1-43, and it released all its dye with exhaustive stimulation (Fig. 1a3). This is quantified in Fig. 1a4 which shows that the fluorescence of bouton 2 fell to background after stimulation. In contrast, boutons 1 and 3 failed to take up any dye during five action potentials, and therefore remained at background throughout the experiment.

The stimulus-induced fluorescence loss in 272 boutons is plotted as a histogram in Fig. 1c. The appearance of discrete peaks indicates the quantal nature of staining following the minimal stimulation procedure (Ryan et al., 1997; Murthy and Stevens, 1998; Harata et al., 2001a). The overall distribution was fitted well by the sum of individual Gaussian components conforming to expectations of quantal theory (Del Castillo and Katz, 1954) (see Section 2). The first peak represents functional synapses identified by maximal staining, but which failed to take up FM1-43 during the 5 APs of the minimal-staining protocol. The second and third peaks consist of synapses that loaded only one or two vesicles, respectively. The spacing between successive peaks, 500 FITC equivalents, corresponds to the average fluorescence of a single synaptic vesicle ($\bar{q}$). Based on this quantal analysis, the 564 FITC equivalents measured in bouton 2 (Fig. 1c) represented a single synaptic vesicle labeled with FM1-43.

As an independent check on quantal size, we labeled

extracellular neuronal plasma membrane with the same concentration of FM1-43 that we used in our vesicle loading experiments. We calculated that 500 FITC equivalents represent the number of FM1-43 molecules that incorporate into 1684 nm^2 of lipid membrane surface area, an area that corresponds to a sphere with a diameter of 24 nm. Our measurements of electron microscopic images indicated that the inner diameter of synaptic vesicles was close to 24 nm (data not shown). This biophysical measurement provides independent confirmation that the spacing between each quantal peak represents the fluorescence of a single vesicle.

As a further check, we estimated the size of the total recycling pool by dividing the fluorescence produced with maximal loading (14,450 ± 450 FITC equivalents, $n = 272$, Fig. 1d) (mean ± s.e.m here and throughout) by the average quantal size $\bar{q}$. The pool size was broadly distributed with an average of 28.9 vesicles and fell within the range of previous estimates obtained by FM1-43 loading (Ryan et al., 1997; Murthy and Stevens, 1999). Harata et al. (2001a) stained equivalent hippocampal cultures with a maximal-staining protocol, photoconverted the vesicles, and used the photoconversion efficiency to estimate the total number of recycling vesicles. These experiments estimated the total recycling pool size of hippocampal presynaptic terminals (photoconversion-positive vesicles) to be 30, in excellent agreement with the present estimate of 28.9 vesicles. This provided a further verification of the idea that the putative quantal unit (500 FITC equivalents) represents the FM1-43 fluorescence of a single synaptic vesicle.

From the preceding quantal analysis, we can estimate the probability of vesicular loading and total recycling pool size. The relative heights of the Gaussian peaks reflect the fact that the loading probability was relatively low, as expected for CA3–CA1 synapses (Rosenmund et al., 1993; Murthy et al., 1997). Indeed, at the great majority of synapses, 5 APs failed to label even a single vesicle. The average loading probability can be calculated by assuming that all synapses have an equal likelihood to exocytosis given an action potential and that successful vesicle loading obeys binomial statistics. Our best-fitted Gaussian curves corresponded to a loading probability of 0.05. The loading probability is conceptually different than the probability of release per bouton ($P_{r/b}$): the loading probability is an underestimate if multiple fusions of a single vesicle each contribute to $P_{r/b}$, but only once to FM dye loading, or if successful fusion events do not couple perfectly with a corresponding endocytotic event.

3.2. Single action potentials release subquantal amounts of dye from single vesicles

Minimal staining and improvements in imaging methods allowed us to monitor the de-staining of indi-

vidual vesicles during repetitive stimulation (Fig. 2). For the remainder of this study, we restricted our analysis to boutons whose total $\Delta F_{\max}$ was within the shaded area of the histogram (Fig. 2f), which represents the range of total fluorescence losses that correspond to one vesicle with >95% certainty (see Section 2). We monitored the exocytosis of single vesicles following single action potentials (Fig. 2). The quantal size in these experiments was 488 FTIC equivalents, very close to that of the experiments comprising Fig. 1. The stimulation rate of 0.125 Hz, allowed enough time between successive APs to permit complete dye departitioning following an individual fusion event. To minimize decay of the single vesicle signal by photobleaching, only 121 images were acquired, enough for 20 APs plus initial and final baselines. After the 20 stimuli, image acquisition was interrupted and 600 stimuli at 10 Hz were applied to completely release any remaining dye in the vesicle (Fig. 2a). Some single vesicles released a full quantum of dye in response to 1 AP (Figs. 2b1, b2), seen as an immediate, step-wise decrease in fluorescence whose amplitude was 100% of the quantal amplitude q (Fig. 2c). Near-complete loss of the punctate fluorescence in 1 AP was consistent with the complete collapse of the vesicle into the plasma membrane. However, we cannot rule out that the possibility that a fusion pore remained patent for long enough to allow all the dye molecules to escape, but then subsequently closed.

Recordings like Fig. 2c were rare ($n = 3$). In most cases, vesicle fluorescence dropped in response to at least one of the 20 APs, but nevertheless fell far short of the final level measured after massive stimulation (Fig. 2e). This indicated a subquantal loss of dye (Figs. 2d1–d3), presumably arising from a fusion event that did not result in complete collapse. A histogram of fluorescence loss from single vesicles after all 20 action potentials emphasizes the predominance of cases where only a fraction of the dye was lost (Fig. 2g, mean, $0.67q$, $n = 20$). The simplest interpretation is that most fusion events did not result in complete collapse, but instead were followed by rapid endocytosis that allowed a portion of the dye to be retained.

3.3. Analysis of dye loss during single fusion events

We analyzed individual fusion events to determine both the timing and magnitude of dye loss in response to single APs (Fig. 3). Fig. 3a shows the fluorescence signal from a vesicle making two distinct fusions. Both fusion events were well-resolved above the noise, releasing >100 FITC equivalents. All single vesicle traces obtained during low-frequency stimulation were fit with a staircase function in order to estimate both the APs at which the events occurred and the magnitude of FM1-43 loss (see Section 2). If one vesicle were responsible for both fusions and the second-fusion event were simi-

lar to the first, one would expect (1) the absolute amount of dye lost in the second fusion to be less than that in the first fusion and (2) a similar fraction of the remaining dye to escape in both fusions. Our data are consistent with both these predictions (Fig. 3c, d). On average, the fraction of dye lost in the second fusion ($0.30q$) was significantly smaller than the first ($0.48q$) (t-test, $P < 0.05$), whereas the relative amounts of dye lost in the second fusions ($0.42q'$, where q' represents the fraction of dye left after the first event) were not significantly different from the first (t-test, $P > 0.5$).

When the data on fractional quantal loss during first and second events were pooled together in a single histogram (Fig. 3b), the results were consistent with the concept of two distinct modes of fusion, one that retains dye (gray bars) and another that leads to the complete loss of the quantum (black bar at unity).

3.4. Analysis of timing of individual fusion events

Our staircase fit of the data allowed us to estimate the first fusion latency of single synaptic vesicles (Fig. 3e). On average, the first resolvable release of dye was detected only 4.9 stimuli after the onset of stimulation ($n = 19$), the small number of APs suggesting that these vesicles were ready for immediate use. In traces where a second-fusion event was resolvable ($n = 8$) (e.g. Fig. 3a), we also determined a second-fusion latency (interval between the first and second fusions) (Fig. 3e). This averaged 7.1 stimulus intervals, corresponding to a mean "reuse time" of 57 s. Because the plateaus between subquantal steps lasted so long, typically 20-fold greater than the time constant for dye departitioning from surface membrane (2.5 s), we could also exclude the idea that FM dye released from vesicles during fusion became trapped in the synaptic cleft.

As seen in a plot of cumulative probability (Fig. 3e), the latency to the first event was roughly exponentially distributed, conforming to a geometric function (black smooth curve) with a release probability per stimulus ($P_{\text{r/v at 0.125 Hz}}$) of 0.20. The relatively high release probability was consistent with the lack of any boutons that completely failed to release at least some their single vesicle's worth of dye content during the course of 20 stimuli. The cumulative distribution of latency to second fusion was significantly different from that of the first fusion (Kolmogorov–Smirnov test, $P < 0.01$), being distinguished by a clearly sigmoid onset. In order to fit this aspect, we assumed that the second release conformed to the same statistics as first fusion, but only after repriming the vesicle, described with an exponentially distributed interval (τ_{reprime}, see Section 2 for definition). The best-fit curve (Fig. 3e, gray smooth curve) was characterized by a $\tau_{\text{reprime at 0.125 Hz}}$ of 23 s. In this simple model, the combination of fusion pore open time, repriming time, and the stochastic probability of release

accounted for the overall reuse time (57 s). The existence of a significant delay before second-fusion was supported by an analysis of the mean time-course of single vesicle de-staining (Fig. 3f). Single vesicle fluorescence signals were time-aligned at their first detectable fusion before averaging. After its initial rapid drop, the average single vesicle response displayed a plateau for a few stimulus intervals, before undergoing a delayed increase in rate of fluorescence loss with continued stimulation.

3.5. Ruling out partial loading and endosomal splitting

The asymmetry between loading, which appears to be quantal, and unloading, which is mostly subquantal, can be accounted for by the rapid rate of dye partitioning from aqueous solution into membrane relative to the much slower dissociation rate (Schote and Seelig, 1998; Cochilla et al., 1999; Neves and Lagnado, 1999). Thus, our results are compatible with a pathway for access to the vesicle inner surface that is at least partly aqueous. We also considered an alternative hypothesis—that a subpopulation of vesicles was partially stained, and that the subquantal losses of fluorescence arose from the full collapse of these vesicles. For this scenario to be true, it would be necessary to find significant subquantal peaks in the histograms of dye loading, interspersed between the main quantal peaks, which were separated by fluorescence differences expected for single vesicles as previously discussed. To assess the possible contribution of such subquantal peaks, we fitted the 10 AP data with five gaussians and constrained the quantal size to be <300 FITC equivalents. The best fit yielded a quantal size of 253 FITC equivalents (Fig. 4b), but failed to improve the quality of fit relative to that obtained with only three gaussians (Fig. 4a). Most importantly, even after imposing the five gaussian fit, the area of the subquantal gaussian peaks was extremely small relative to the regular peaks. (In fact, the successive gaussian amplitudes (v_0, v_1, etc.) did not decrease monotonically with peak number, but oscillated, in contradiction to what would be expected for a binomial process like that envisioned for quantal uptake; this buttressed the conclusion that the fundamental quantum of dye uptake was ~500 FITC equivalents, not ~250). Relative to the weight of the peak at ~500 FITC equivalents, any contribution of intermediate peaks (putative partially stained vesicles) would be extremely small. A number of arguments against endosomal splitting (see below) also argue against subquantal loading.

Another issue concerns the idea that dye may be internalized in full quantal units but then subdivided into smaller packets that are manifested in individual de-staining events. In preparations like the frog neuromuscular junction, endocytosis leads to proto-vesicular structures that fuse with internal membrane compart-
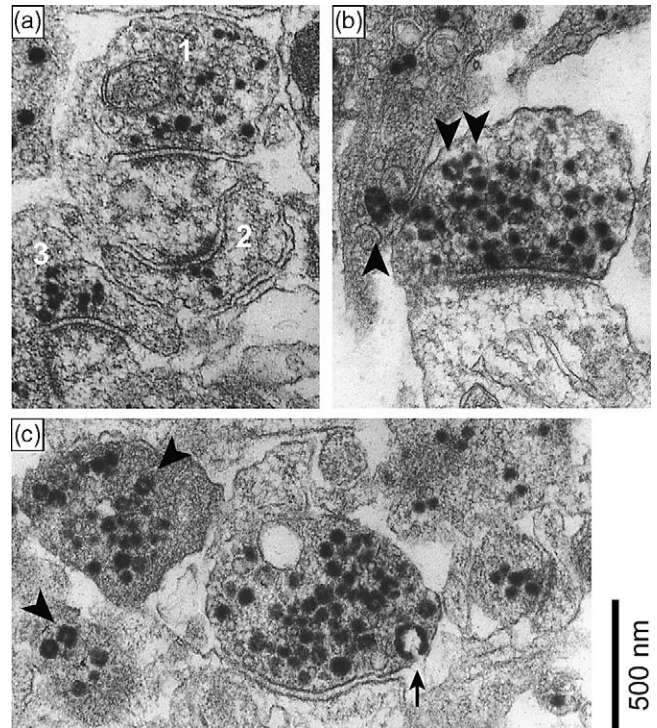

Fig. 5. Electron microscopy shows that endosomal profiles were rarely found in hippocampal terminals even after extensive stimulation. (a) Photoconversion-positive structures in the majority of EM sections were small, round synaptic vesicles only (boutons 1–3) (138 out of 185 boutons, 75%). (b, c) Endosomal profiles (arrowheads) were present in the remaining boutons. They were larger than vesicles, round, and contained electron-dense product in the periphery surrounding an electron-lucent center. Although serial sectioning was not performed, the extremely low incidence of endosomal profiles suggested that endosomal trafficking would have had little influence on the quantal parameters, particularly after minimal loading. For completeness, we show an example of an endosomal profile that directly connects with the plasma membrane (arrow in c), which appeared to be made up of several vesicles' worth of membrane (cf. Takei et al., 1996; Richards et al., 2000). These were rare (only 1 out of 185 boutons), and would likely have corresponded to one of the higher order ($k \geq 2$) quantal peaks in the histogram of fluorescence uptake, out of the purview of our unitary analysis.

ments known as endosomes (Heuser and Reese, 1973). The prevalence of endosomal trafficking at small central synapses has been discounted in previous experiments with FM1-43 (Murthy and Stevens, 1998). Nonetheless, we thought it prudent to reconsider a scenario in which a single dye-stained proto-vesicle budded from the plasma membrane, fused with an endosome, and then gave rise to two or more partly stained synaptic vesicles, which then fused independently. In such an "endosomal splitting" scheme, a single quantum of dye uptake might eventually give rise to subquantal steps of fluorescence loss, even if classical full collapse were the mechanism of fusion.

Multiple lines of evidence rendered this interpretation unlikely, if not untenable.

First, contrary to the traditional picture of vesicle cyc-

ling, the generality of endosomal dilution was ruled out by our finding that fully stained vesicles sometimes underwent complete loss of fluorescence following a single action potential (Fig. 2b, c, and Fig. 7).

Second, it is likely that only a small proportion of dye-stained membrane in hippocampal terminals passes through endosomes, given their rarity even after much heavier stimulation than in this study (Fig. 5; Harata and Tsien, 2001; Schikorski and Stevens, 2001). We estimated the number of endosomal structures with FM dye photoconversion and electron microscopy (Harata et al., 2001b). Hippocampal terminals were allowed to take up FM dye during and up to 1 min after extensive field stimulation (20 Hz, 60 s), then fixed after a variable interval and photoconverted in the presence of 3,3′-diaminobenzidine (DAB) to form an electron-dense product that could be clearly detected under EM. Endosomal profiles were identified as round- or horseshoe-shaped profiles with electron-dense product in a peripheral band around a clear central lumen. Their diameter (60–100 nm) was significantly greater than that of SVs (40 nm). As illustrated in Fig. 5, the endosomal profiles were clearly identifiable in a minority of EM sections, but were greatly outnumbered by SV profiles in the same sections (data that follow are given on a per section basis). With a 1 min interval after stimulation, PC-positive SVs numbered 15.5 ± 0.91 per bouton, while PC-positive endosomal profiles numbered 0.66 ± 0.13 per bouton (range 0–15, $n = 185$). Three-quarters of the sections lacked any hint of an endosome-like structure. If these observations for single EM sections are referred to the number of functional quanta in this study (~29), to put the data on a whole terminal basis, one would expect only ~1.2 endosomal structures per nerve terminal even after heavy stimulation; a large fraction of presynapses would lack such structures altogether. Given the known rates of membrane traffic through endosomal structures, determined at the NMJ and other secretory systems, it is difficult to see how the few endosomes could give rise to significant splitting up of the unitary dye uptake.

Third, this scenario is at odds with the findings that second fusions release a significantly smaller absolute amount of dye (Fig. 3c) but a similar fraction of remaining dye (Fig. 3d). The scenario of endosomal splitting would predict that, on average, the absolute amounts of dye loss would be equal, contrary to our data.

Fourth, the endosomal splitting/classical fusion scenario predicts no difference in the time course of de-staining for partially and fully dye-filled vesicles. However, our data suggested that the subquantal drops in fluorescence settled more quickly than the full quantal decreases (Fig. 4c; see Section 4 for further interpretation).

Fifth, we observed an extra delay between the initial fluorescence step and a second step (Fig. 3e), contradicting what would be expected for independent fusions
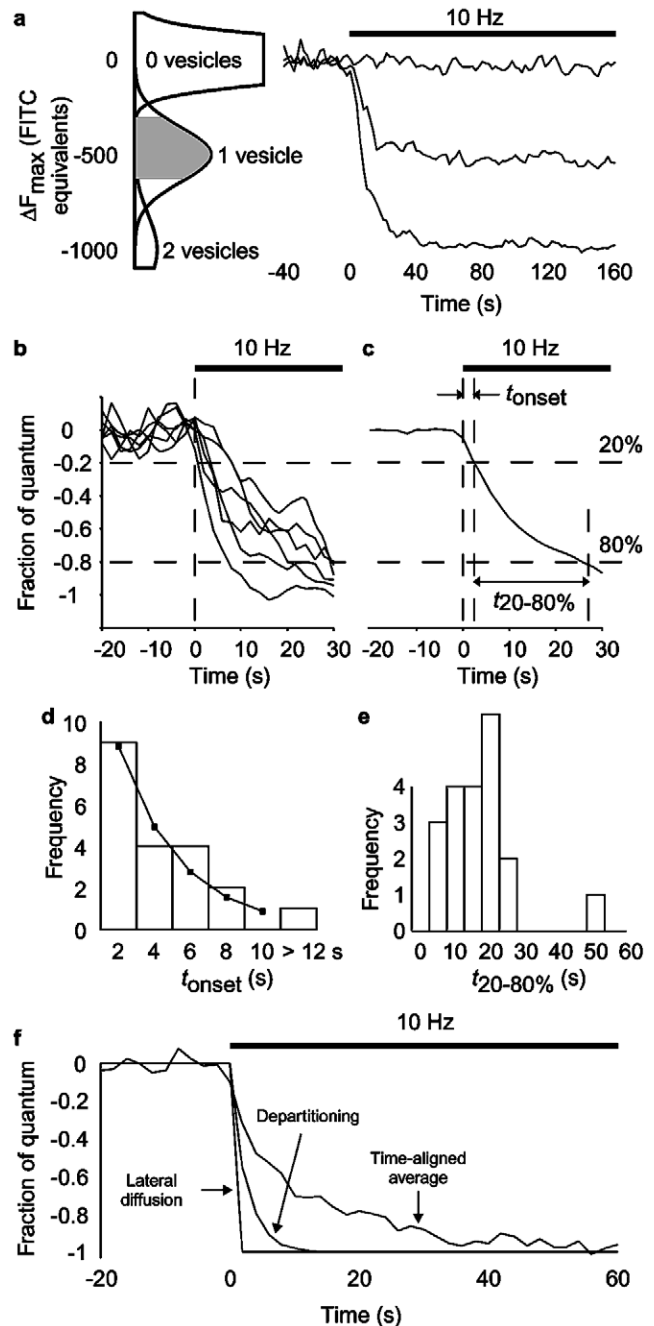

Fig. 6. Single vesicles loaded during minimal stimulation fuse multiple times during 10 Hz stimulation, and remain in the readily releasable pool after first fusion. (a) Fluorescence signals from individual boutons containing 0, 1, or 2 vesicles during 10 Hz stimulation. Shaded area in histogram: single vesicles with >95% confidence. (b) Time-expanded records of single vesicles de-staining. (c) Average of 20 singles with analysis scheme: time from stimulus initiation to >20% dye loss (t_{onset}), time from >20% to >80% dye loss ($t_{20–80\%}$). (d) Histogram of t_{onset} (4.6 ± 1.0 s, $n = 20$). Solid line, fitted geometric distribution with probability of release per vesicle ($P_{r/v\ @\ 10\ Hz}$) = 0.03. (e) Histogram of $t_{20–80\%}$. (f) Average of time-aligned traces ($n = 20$; normalized, aligned to t_{onset}, and averaged). A single exponential fit gave $\tau = 10.3$ s, much slower than time courses of FM1-43 release predicted by ideal dye departitioning or ideal lateral diffusion, indicating that multiple fusion events are probably required to release the full quantum. From Aravanis et al. (2003), with permission.
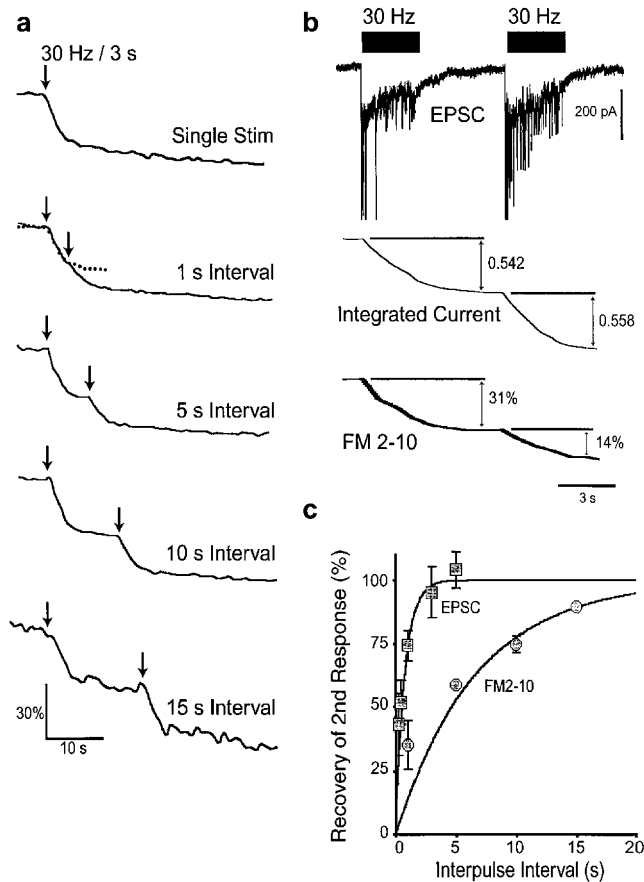
Fig. 7. Vesicles of the RRP are capable of multiple release events during Ca^{2+}-dependent stimulation. (a) De-staining of FM2-10 associated with bursts of activity driven by electrical stimulation (30 Hz for 3 s, onset indicated by downward arrow). A single burst, chosen to cause near-complete release of RRP vesicles, caused FM2-10 de-staining corresponding to ~30% of the total recycling pool ($n = 72$). A second identical burst, following 1 s after the first one, gave rise to much less FM2-10 fluorescence loss (10% of the total pool, $n = 82$). For reference, the dotted line gives the time course of fluorescence loss during a single burst. Additional traces show the effect of increasing the interval between the bursts of stimuli. Expressed as a percentage of the total pool, the release of FM2-10 during a second stimulus recovers to 13% after 5 s ($n = 123$), 18% at 10 s ($n = 131$), and 27% at 15 s ($n = 122$). (b) Comparison between the recovery of postsynaptic whole-cell currents and FM2-10 fluorescence loss during the interval between bursts of electrical stimulation. Ca^{2+}-dependent recovery of the ability to support neurotransmitter release was monitored by recording the postsynaptic response in a follower cell while focally applying bursts of extracellular stimuli to the cell body of a nearby neuron. The initial volley of action potentials elicited vigorous neurotransmitter release (EPSC; upper trace). As seen in the running integral of current signal (middle trace), the initial response (0.542 pC) was closely matched by the second response (0.558 pC). In contrast, the corresponding drop in FM2-10 fluorescence (lower trace) was 31% of the total recycling pool for the first stimulus but only 14% for the second. (c) Following depletion by electrical stimulation, the rate of recovery of the availability of vesicles to release neurotransmitter greatly exceeded the rate of repopulation of RRP from the RP. The percentage of recovery of neurotransmitter release was calculated as the ratio of integrated currents from the second and first responses (for intervals of 250 ms, $n = 2$; 500 ms, $n = 3$; 1 s, $n = 5$; 3 s, $n = 5$; 5 s, $n = 3$; 10 s, $n = 3$; n values indicate the number of cells contributing to the pooled electrophysiological data). The percentage of recovery of FM2-10 de-staining was obtained from traces where double challenges were applied by calculating the ratio of the second and first fluorescence changes, with appropriate correction for the decline in FM2-10 fluorescence that would have occurred after only a single challenge (Fig. 7a; for intervals of 1 s, $n = 82$; 5 s, $n = 123$; 10 s, $n = 131$; 15 s, $n = 122$. The recovery of neurotransmitter release was fitted with a single exponential ($\tau < 1$ s, $R^2 = 0.96$). From Pyle et al. (2000), with permission.

of the daughter vesicles that had arisen from endosomal splitting.

Sixth, the number of successive fusions is far in excess of what would be expected from the classically predicted behavior of partially stained daughter vesicles (see Fig. 4 for details).

In view of these lines of evidence, it is difficult if not impossible to explain our data by a combination of endosomal splitting and classical fusion by complete collapse. Note that several of these arguments (first, third, fourth, and fifth) also weigh against the scenario of partial loading of a single vesicle.

3.6. At physiological frequencies, multiple fusion events are required to de-stain single synaptic vesicles

The preceding analysis was helped by the use of a low stimulation rate, but the question naturally arises as to how single vesicles behave at higher frequencies of stimulation, as encountered under physiological conditions. Fig. 6a shows records during 10 Hz stimulation from boutons characterized as containing zero, one, or two FM1-43 stained vesicles, based on the same selection criteria described above. Each single vesicle signal was analyzed to determine the time between the onset

of stimulation and its first exocytosis ($t_{onset} \equiv t_{20\%}$) and the time for quantal loss ($t_{20–80\%}$) (Fig. 6b, c). For most terminals stimulated at 10 Hz (65%), t_{onset} of the only labeled vesicle was 4 s or less (Fig. 6d). Since these vesicles began to exocytose during the first 40 APs, they largely belonged to the pool of vesicles available for immediate use, a subset of vesicles often called the readily releasable pool (RRP) (Rosenmund and Stevens, 1996; Murthy and Stevens, 1999). The RRP in these terminals comprises between one-third and one-fourth of the total number of vesicles available for fusion (Murthy and Stevens, 1999; Pyle et al., 2000). Therefore, if the single loaded vesicle mixed randomly in the vesicle pool of the terminal, we would have expected less than ~30% of single vesicles to reside in the RRP. The immediate availability of the single dye-labeled vesicle suggested that it was labeled and retrieved at or near the active zone and kept there for the duration of 15-min wash in zero Ca^{2+} solution.

By fitting a geometric distribution to the distribution

of values of t_{onset}, we estimated the probability of fusion for a single vesicle at 10 Hz ($P_{r/v \text{ at } 10 \text{ Hz}}$) to be 0.03. If one assumes that all vesicles in the RRP have the same probability of fusion given an action potential, a rough estimate of the terminal's probability of release ($P_{r/b \text{ at } 10 \text{ Hz}} = 0.21$) is made by multiplying $P_{r/v \text{ at } 10 \text{ Hz}}$ by the approximate number of vesicles in the RRP (Pyle et al., 2000). This estimate could not be compared to the probability of loading because the probability of loading was estimated from all functional synapses in a field of view and assumed that the probability of release for all of the terminals was equal. $P_{r/v \text{ at } 10 \text{ Hz}}$ was estimated only from those boutons that successfully loaded a vesicle, a set of terminals expected to have a higher than average probability of release.

In contrast to the brief initial latency of single vesicles, $t_{20-80\%}$ was relatively long, averaging 16.9 ± 2.3 s (mean $\pm$ s.d., $n = 20$) (Fig. 6e). This was not consistent with a model of exocytosis in which fusion always leads to complete collapse. In that case, the longest de-staining time ($t_{20-80\%}$) of a single vesicle would be 3.5 s, based on the measured kinetics of FM1-43 departitioning from neuronal membranes (Klingauf et al., 1998). This disparity was underscored by analysis of the average time course of single vesicle de-staining after time aligning individual records to the point of t_{onset} (Fig. 6f). The average record was best-fit with a single exponential with $\tau = 10.3$ s, much slower than the $\tau_{departition} = 2.5$ s predicted for complete collapse with departitioning (Klingauf et al., 1998), and even further out of line with the $\tau_{lateral} \sim 10$ ms predicted for lateral diffusion (Zenisek et al., 2002) (smooth curves, Fig. 5f). These large differences implied that the vesicle failed to undergo complete collapse, but remained in a structural form that allowed subsequent rapid retrieval and dye retention for at least several seconds. Complete de-staining of the vesicle was achieved ultimately, but was likely to require additional exocytotic events (Pyle et al., 2000). Thus, the findings with 10 Hz stimulation were very compatible with those obtained at 0.125 Hz (Figs. 2 and 3).

4. Discussion

Improvements in instrumentation and experimental protocols enabled us to track the real-time de-staining of single FM-labeled vesicles in small central terminals. In order to maximize the fluorescent signal, we used a high numerical aperture lens (1.3 NA) and imaged on to an intensified CCD camera. To minimize the effects of vesicle z-position variation, auto-fluorescence, and background fluorescence from non-vesicular staining, we selected for processes on bare glass and used a lens with a depth of focus of ~1 μm. Since CA3–CA1 hippocampal boutons have diameters <1 μm, most of the light from FM1-43 in vesicles was captured. ROI size was

chosen to be just large enough to be insensitive to small changes in the focus. Capitalizing on these technical improvements, our experiments yielded findings that were surprising in the context of the time-honored scenario for fusion and endocytosis (Heuser and Reese, 1973) and its recent experimental manifestations (Zenisek et al., 2000; 2002). The great majority (85%) of the single FM1-43 labeled vesicles we studied lost only a part of their dye molecules during an individual fusion event. This observation was most simply explained by the prevalence of a fusion process that maintains vesicle integrity, followed by a retrieval process too quick to allow all dye to escape (Fig. 8). Once the fusion event had concluded, the retention of dye in the vesicle interior was measured as a subquantal fluorescence signal. A typical vesicle that underwent such transient fusion was a member of the readily releasable pool, based on the small number of action potentials required to cause its release (Figs. 3e and 6d). After rapid retrieval, such vesicles appeared to remain near the sites of vesicle fusion for some time, as indicated by their ability to support multiple cycles of exocytosis and endocytosis (Figs. 3a and 6e). The mechanism of vesicle reuse applied over the wide range of stimulus frequencies that we have examined (0.125, 10, and 30 Hz).

Our evidence sets limits on how transient the fusion event must be (t_{open}). If FM dye escaped by departitioning from the vesicle lipid and diffusing through an aqueous fusion pore (Klingauf et al., 1998), the average subquantal decrement in FM staining corresponds to a pore open time of <1.4 s. If the FM dye were able to escape by lateral diffusion from the inner leaflet of the vesicle to the outer leaflet of the plasma membrane (Zenisek et al., 2002), lipid continuity must last <10 ms. On a preliminary basis, our data favors the aqueous departitioning as the predominant mechanism. The average time course of events with full quantal loss is plotted in Fig. 4c (triangles). The approach of the fluorescence signal to the baseline is incomplete at 4 s, but only attains its final level at 6 s and beyond, consistent with aqueous departitioning ($\tau = 2.5$ s) as the rate-limiting step. If the mechanism of dye escape were lateral diffusion in the plasma membrane, a much faster time course would have been expected ($\tau \sim 10$ ms, solid gray line). In contrast, the average time course of events with only partial quantal loss (squares) is consistent with a more rapid settling, as would be expected if the vesicles adhered to the same kinetic trajectory of dye loss up to the instant of fusion pore closure (on average, a bit more than one second after the successful stimulus), then kept the remaining dye (maintained level of fluorescence indicated by dashed line). Further work is needed to pin down the time course of fluorescence decrease more precisely, but the evidence to date does not display the rapid fluorescence drop predicted by lateral diffusion.

a Kiss-and-Run Fusion

fully loaded vesicle at rest — 500

first fusion leaves vesicle completely or partially intact → 1 Action Potential

partially loaded vesicle between fusion events — 315

reuse leaves vesicle completely or partially intact → 1 Action Potential

partially loaded vesicle between fusion events — 160

repeated reuse further unloads the vesicle → Additional Action Potentials

multiple fusions release all dye from the vesicle

b Full Quantal Loss

fully loaded vesicle at rest — 500

fusion leads to loss of the full fluorescence quantum → 1 Action Potential

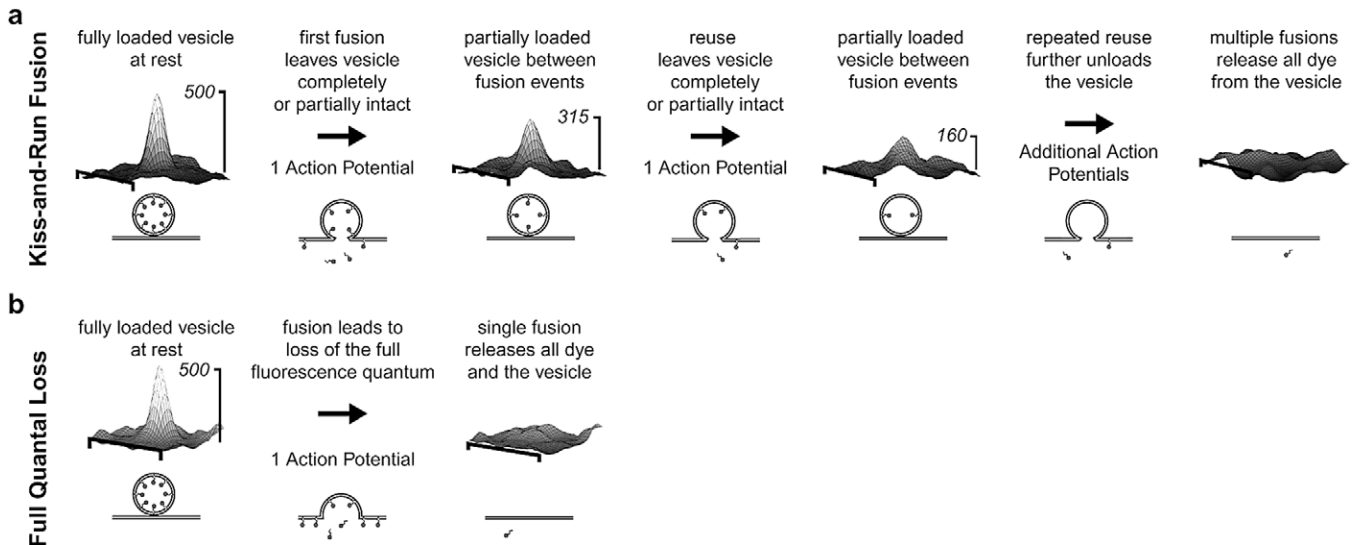single fusion releases all dye and the vesicle

Fig. 8. Contrasting modes of vesicle fusion in a small central presynaptic terminal, implicated by different patterns of FM1-43 de-staining at the single vesicle level. (a) Kiss-and-run fusion, an exocytosis–retrieval process that preserves integrity of a single vesicle and allows its reuse, and (b) full quantal loss, wherein the vesicle completely de-stains, possibly because its membrane rapidly and completely integrates into the plasma membrane. In both cases, the fluorescence signal from a single labeled vesicle is shown as a 3D intensity plot as they proceed along their respective fusion pathways. The horizontal scale bar along each 3D intensity plot represents 6.8 μm; each 3D plot represents the average of five fluorescent images and was filtered for clarity of presentation. In (a), a single labeled vesicle containing FM dye with fluorescence equivalent to ~500 FITC molecules fused in response to a single action potential and lost ~180 FITC equivalents of fluorescence; dye was most likely released by direct aqueous departioning from the vesicle membrane into solution. Because the vesicle pulled back intact from the fusion state, ~315 FITC equivalents remained sequestered until a point 10 stimuli later when the vesicle responded to another single AP and lost an additional 155 FITC equivalents (reuse). The remaining ~160 FITC equivalents of fluorescence were lost still later, while the lumen of the vesicle was opened to extracellular space during application of 600 stimuli (further reuse). (b) A single FM1-43-stained vesicle with fluorescence equivalent to ~500 FITC molecules fused and lost all of its fluorescence in response to a single action potential. One possibility is that all of the dye escapes via full fusional collapse, in line with evidence for this possibility in other secretory systems (Heuser, 1989; Sudhof, 1995; Zenisek et al., 2002). An alternative scenario is that vesicle integrity is maintained but continuity between vesicle lumen and extracellular space lasts long enough to allow dye to escape completely, perhaps due to "compensatory" or "stranded" modes of Gandhi and Stevens.

4.1. Comparisons with other approaches to gauging single vesicle dynamics

It is interesting to compare our results with a recent study by Gandhi and Stevens (2003), who also studied synapses in hippocampal cultures, focusing specifically on very low frequencies of stimulation. Their optical indicator was synaptophluorin, a variant of enhanced green fluorescent protein (EGFP), tuned to be highly pH-sensitive, fused to the luminal end of the vesicle protein synaptobrevin (VAMP). Fusion events at the single vesicle level were registered as a transient increase in vesicle fluorescence, caused by an initial loss of hydrogen ions from the vesicle lumen (relief of synaptophluorin quenching), followed by a decay of fluorescence (re-acidification by the vesicular H^+ pump and restoration of synaptophluorin quenching). This system provided independent evidence for the existence of multiple modes of synaptic vesicular recycling. Two forms of exocytotic event were terminated by long-delayed vesicle retrieval: a slow "compensatory" mode wherein retrieval took place in a time window 8–21 s after the initial fusion, and a "stranded" mode, in which a vesicle was left on the cell surface for an indefinite period until

a subsequent nerve impulse triggered its retrieval. Either one of these recycling modes as defined by Gandhi and Stevens would have given rise to a complete loss of vesicular FM1-43 staining after a single fusion event. Thus, it is reasonable to think that some combination of "compensatory" and "stranded" modes would account for those events where we observed full quantal loss with FM1-43.

Gandhi and Stevens also observed a "kiss-and-run" mode, characterized by a selective fusion pore and a much briefer exocytotic event. The fusion pore was much more passable to Tris than to HEPES, and remained patent for 400–860 ms (the range depending on the time assigned to the re-acidification process after vesicular retrieval). We regard the "kiss-and-run" mode of Gandhi and Stevens as the likely equivalent of the kiss-and-run events seen in our experiments. Our estimated time constant of <1.4 s (and the earlier estimate of ≈ 1 s of Pyle et al. based on other evidence) and their value of 400–860 ms are reasonably close. The prevalence of their kiss-and-run mode, 75% of fusion events at low P_r synapses ($P_{r/b} = 0.2$), is also consistent with the dominance of kiss-and-run that we observed (85% of events).

Other experiments provide additional cross-checks on the equivalency of the fusion modes dubbed "kiss-and-run".

1. In loading experiments, Pyle et al. examined the uptake of FM1-43 caused by a 2-s burst of AP stimulation that turned over the readily-releasable pool. Dye was only present during the 2-s stimulation and then it was immediately washed out of the bath. FM dye loading was unchanged by extending the period of dye exposure for an extra 30 s beyond the stimulation (Pyle et al., 2000). This implied that steady-state loading was achieved within the time frame of Gandhi and Stevens' kiss-and-run events, and in turn, that dye was able to pass through the corresponding fusion pore.
2. In our kinetic analysis of events showing partial loss of a quantum of FM1-43 (Fig. 4c), the fluorescence drop settled within <2 s. Fusion events terminated within 2 s or less would be unambiguously categorized as "kiss-and-run" mode according to the Gandhi–Stevens classification.
3. The results of comparisons between various FM dyes with differing kinetic features also provided support for an aqueous connection between vesicle lumen and external solution that lasted on the order of 1 s. Klingauf et al. (1998) and Pyle et al. compared the behavior of FM1-43 with its short-tailed congener, FM2-10, which departitions with a $\tau = 0.6$ s rather than 2.5 s. In combination with the four-fold faster desorption rate, a fusion pore opening lasting ≈ 1 s was invoked to account for the kinetic differences observed, anticipating the conclusions of Gandhi and Stevens and Aravanis et al. (Aravanis et al., 2003). In hindsight, the desorption rates of the FM dyes were well-suited to provide kinetic information on the time scale of the postulated kiss-and-run events. Vesicles loaded with FM2-10 would be expected to lose nearly all their dye during a kiss-and-run event, not between 1/3 and 1/2, as in the case of FM1-43.

Another important area of comparison is with Zenisek et al. (2002), who used evanescent wave microscopy to study FM1-43 loss from single vesicles in goldfish bipolar terminals. In the great majority of experiments, they saw an abrupt drop in vesicle fluorescence and no lasting dye retention, as if the sole mechanism of dye escape were lateral diffusion. Accordingly, they commented as follows on the hypothesis of incomplete exocytosis at synapses: "We find it hard to imagine how kiss-and-run can be definitively established other than at the level of single vesicles". Now that this challenge has been addressed, it is nonetheless interesting to ask why the results in their system and in small central nerve terminals differ so markedly. One possibility is simply biological variation: their non-mammalian bipolar nerve ter-

minal contains nearly one million vesicles, undergoes nearly continuous transmitter release in vivo, and may have little need for deployment of kiss-and-run (Zenisek et al., 2002). Another idea is that their choice of spatial "outliers" away from the active zone may select for classical full collapse events. Finally, it is the papain treatment they used to remove postsynaptic elements that caused proteolytic damage to presynaptic components and which controls the biophysics of exo/endocytosis, comparable to effects of α-latrotoxin.

From a broader perspective, the multiple approaches discussed above are inherently complementary. Vesicular entry of pH buffers specifically reflects passage through an aqueous pathway and provides the best method to date for gauging the properties of a kiss-and-run fusion pore, but all the observed kinetic behavior is complicated by the extra step of luminal re-acidification by the vesicular proton pump, whose properties may vary from one experimental condition to another and from one vesicle to the next. Evanescent wave microscopy provides the best z-axis resolution of any approach, but this can be a disadvantage in assigning fluorescence signals to changes in the positions or contents of multiple vesicles; additionally, it is difficult to study single vesicles at the active zone itself (Zenisek et al., 2002). The interpretation of FM1-43 experiments is made more complex because of the possibility of alternative routes for dye molecules to escape, although this can be turned to advantage under some circumstances, particularly at the single vesicle level.

4.2. Lessons from tracking single vesicles over many stimuli

One special feature of our approach is the ability to track an individual vesicle over many stimuli and at varying stimulus rates. This allowed us to go beyond the observation of brief exocytotic events, to ask about the fate of the fusing vesicle after its quick retrieval. How is the rapidly retrieved vesicle reintegrated into the overall pool, and is it actually reused? Single FM1-43 loaded vesicles made a second fusion not long after the first fusion, on average only seven stimuli later at 0.125 Hz. Because seven action potentials could produce only a small number of fusion events overall, the second fusion of the labeled vesicle must have been either the very next successful fusion event or one close on its heels, as expected for a privileged resident of the RRP. A distinct, but perhaps causally related observation concerns the first fusions of dye-loaded vesicles. These occurred on average remarkably soon after the initiation of stimulation—within <40 APs at 10 Hz and within <5 APs at 0.125 Hz. In other words, after the minimal-staining protocol labeled a single RRP vesicle, and even after a wash in 0 Ca^{2+} solution for >15 min, the same vesicle was found in the RRP once again. Although a precise

spatial localization would be beyond the resolution of light microscopy, the clear implication is that the labeled vesicle remained in the RRP for the entire intervening period. Together, these observations point to a significant revision of the prevailing view of the presynaptic terminal, wherein vesicles at the active zone occupy the front of a queue and newly endocytosed vesicles join the back of the queue, waiting their turn for fusion in orderly fashion. Instead, our experiments support the idea that a vesicle undergoing rapid fusion–retrieval is predisposed to rejoin the readily releasable pool, effectively cutting in line.

4.3. Evidence that reused vesicles release neurotransmitter

When a vesicle fuses repeatedly, as judged by successive losses of FM1-43 fluorescence, does it also support repeated release of neurotransmitter? Our previous work approached this fundamental question by comparing electrophysiologically monitored neurotransmission with vesicle turnover tracked by the rapidly desorbing dye FM2-10 (Pyle et al., 2000). Because the transmitter content of vesicles at hippocampal synapses is rapidly restored, maintaining unitary discharge properties even at high stimulus rates (Zhou et al., 2000), the amount of neurotransmitter released is directly related to the number of fusion events, irrespective of whether the vesicles are fusing for the first time or being reused. In contrast, vesicles labeled with FM2-10 would be expected to release the great majority of their dye content during the first-fusion event (indicated by a comparison of FM2-10 loading and unloading, Fig. 1 in Pyle et al. (2000); see also Sara et al. (2002)). This led to a testable prediction: a vesicle fusing for the first time will release neurotransmitter and FM2-10, but the same vesicle fusing again may release neurotransmitter but little or no additional FM2-10.

Fig. 7 reviews evidence that this was actually the case in transmission among hippocampal neurons (Pyle et al., 2000). Changes in postsynaptic currents and FM2-10 fluorescence were monitored separately during the application of the same patterns of extracellular stimulation (single 3-s bursts of 30 Hz stimulation, or pairs of such bursts separated by a variable interval). In the FM fluorescence experiments, the stimuli were applied through field electrodes and evoked widespread de-staining of fluorescent puncta within areas of study; in the whole-cell recordings, synaptic connections onto the target cell were activated by focal extracellular stimulation of a single presynaptic neuron. As the interval between the bursts of electrical stimulation was progressively lengthened, we observed a gradual recovery of the size of the second response as a percentage of the first. The time course of recovery was quite different for FM2-10 de-staining (Fig. 7a) and postsynaptic current (Fig. 7c). For example, with an interval of 5 s, the postsynaptic current was just as great during the second stimulation as during the first, whereas the release of FM2-10 had only recovered by 50% (Figs. 7b, c). The complete recovery of postsynaptic current showed that the second round of fusion was nevertheless associated with a full measure of neurotransmitter secretion, just as expected (Zhou et al., 2000). Notably, the deficit in the dye signal in the second response indicated that less than half of the fusion events arose from vesicles fusing for the first time. At least 50% of the fusion events must be attributed to vesicles which had already lost most or all of their initial load of FM2-10 dye, but were able to refill with neurotransmitter. This form of vesicle reuse implied that single vesicles were able to fuse transiently and repeatedly, presumably while remaining resident at the active zone. At even longer intervals, the RRP vesicles that have lost FM2-10 were displaced by fresh vesicles from the reserve pool that are fully loaded with dye, thereby supporting the recovery of the stimulus-evoked de-staining.

Now that transient and repeated fusion has been directly observed in our single vesicle experiments, it is all the more interesting to ask about the functional significance of these non-classical phenomena. Working together, kiss-and-run and reuse may allow the efficient use of a small number of RRP vesicles, thereby maximizing the storehouse of vesicles maintained in readiness for recruitment with intense activity (Pyle et al., 2000; Sara et al., 2002). In line with this suggestion, the single vesicle studies at small central terminals have provided convincing evidence, applicable specifically to vesicles long-resident in the RRP, that kiss-and-run predominates over other modes of fusion. Further work is needed to determine the extent to which vesicles that are newly recruited to the RRP undergo rapid fusion–retrieval and reuse. Indeed, studies of multi-vesicular dynamics suggest that under sustained intense stimulation and all-out vesicular mobilization, the mode of fusion–retrieval may shift to favor classical mechanisms of full collapse and de novo re-creation of vesicles (Miller and Heuser, 1984; Ryan et al., 1993; Neves and Lagnado, 1999; Stevens and Wesseling, 1999; Pyle et al., 2000). A combination of rapid fusion–retrieval and classical exo/endocytosis would be well-suited for patterns of firing found in the hippocampus in vivo, in which low rates of spiking are punctuated by episodic bursts of activity (Kubie et al., 1990; Dobrunz and Stevens, 1999). A pressing challenge is to extend the study of modes of fusion and retrieval to all the functional vesicles in the nerve terminal, not just long-time sojourners in the readily releasable pool.

References

Aravanis, A.M., Pyle, J.L., Tsien, R.W., 2003. Single synaptic vesicles fusing transiently and successively without loss of identity. Nature 423, 643–647.

Ceccarelli, B., Hurlbut, W.P., Mauro, A., 1973. Turnover of transmitter and synaptic vesicles at the frog neuromuscular junction. J. Cell Biol. 57, 499–524.

Cochilla, A.J., Angleson, J.K., Betz, W.J., 1999. Monitoring secretory membrane with FM1-43 fluorescence. Annu. Rev. Neurosci. 22, 1–10.

Deisseroth, K., Bito, H., Tsien, R.W., 1996. Signaling from synapse to nucleus: postsynaptic CREB phosphorylation during multiple forms of hippocampal synaptic plasticity. Neuron 16, 89–101.

Del Castillo, J., Katz, B., 1954. Quantal components of the end plate potential. J. Physiol. (Lond.) 124, 560–573.

Dobrunz, L.E., Stevens, C.F., 1997. Heterogeneity of release probability, facilitation, and depletion at central synapses. Neuron 18, 995–1008.

Dobrunz, L.E., Stevens, C.F., 1999. Response of hippocampal synapses to natural stimulation patterns. Neuron 22, 157–166.

Gandhi, S.P., Stevens, C.F., 2003. Three modes of synaptic vesicular recycling revealed by single-vesicle imaging. Nature 423, 607–613.

Harata, N., Pyle, J.L., Aravanis, A.M., Mozhayeva, M., Kavalali, E.T., Tsien, R.W., 2001a. Limited numbers of recycling vesicles in small CNS nerve terminals: implications for neural signaling and vesicular cycling. Trends Neurosci. 24, 637–643.

Harata, N., Ryan, T.A., Smith, S.J., Buchanan, J., Tsien, R.W., 2001b. Visualizing recycling synaptic vesicles in hippocampal neurons by FM 1-43 photoconversion. Proc. Natl. Acad. Sci. USA 98, 12748–12753.

Harata, N., Tsien, R.W., 2001. Properties of endosomal profiles in hippocampal nerve terminals stained by FM dye photoconversion. Soc. Neurosci. Abstr.

Harris, K.M., Sultan, P., 1995. Variation in the number, location and size of synaptic vesicles provides an anatomical basis for the non-uniform probability of release at hippocampal CA1 synapses. Neuropharmacology 34, 1387–1395.

Heuser, J., 1989. The role of coated vesicles in recycling of synaptic vesicle membrane. Cell Biol. Int. Rep. 13, 1063–1076.

Heuser, J.E., Reese, T.S., 1973. Evidence for recycling of synaptic vesicle membrane during transmitter release at the frog neuromuscular junction. J. Cell Biol. 57, 315–344.

Kim, K.T., Koh, D.S., Hille, B., 2000. Loading of oxidizable transmitters into secretory vesicles permits carbon-fiber amperometry. J. Neurosci. 20, RC101.

Klingauf, J., Kavalali, E.T., Tsien, R.W., 1998. Kinetics and regulation of fast endocytosis at hippocampal synapses. Nature 394, 581–585.

Klyachko, V.A., Jackson, M.B., 2002. Capacitance steps and fusion pores of small and large-dense-core vesicles in nerve terminals. Nature 418, 89–92.

Kubie, J.L., Muller, R.U., Bostock, E., 1990. Spatial firing properties of hippocampal theta cells. J. Neurosci. 10, 1110–1123.

Liu, G., Tsien, R.W., 1995. Properties of synaptic transmission at single hippocampal synaptic boutons. Nature 375, 404–408.

Malgaroli, A., Tsien, R.W., 1992. Glutamate-induced long-term potentiation of the frequency of miniature synaptic currents in cultured hippocampal neurons. Nature 357, 134–139.

Marsh, M., Mcmahon, H.T., 1999. The structural era of endocytosis. Science 285, 215–220.

Miller, T.M., Heuser, J.E., 1984. Endocytosis of synaptic vesicle membrane at the frog neuromuscular junction. J. Cell Biol. 98, 685–698.

Murthy, V.N., Sejnowski, T.J., Stevens, C.F., 1997. Heterogeneous release properties of visualized individual hippocampal synapses. Neuron 18, 599–612.

Murthy, V.N., Stevens, C.F., 1998. Synaptic vesicles retain their identity through the endocytic cycle. Nature 392, 497–501.

Murthy, V.N., Stevens, C.F., 1999. Reversal of synaptic vesicle docking at central synapses. Nat. Neurosci. 2, 503–507.

Neves, G., Lagnado, L., 1999. The kinetics of exocytosis and endocytosis in the synaptic terminal of goldfish retinal bipolar cells. J. Physiol. (Lond.) 515, 181–202.

Palfrey, H.C., Artalejo, C.R., 1998. Vesicle recycling revisited: rapid endocytosis may be the first step. Neuroscience 83, 969–989.

Pyle, J.L., Kavalali, E.T., Piedras-Renteria, E.S., Tsien, R.W., 2000. Rapid reuse of readily releasable pool vesicles at hippocampal synapses. Neuron 28, 221–231.

Ribchester, R.R., Mao, F., Betz, W.J., 1994. Optical measurements of activity-dependent membrane recycling in motor nerve terminals of mammalian skeletal muscle. Proc. R. Soc. Lond., B Biol. Sci. 255, 61–66.

Richards, D.A., Guatimosim, C., Betz, W.J., 2000. Two endocytic recycling routes selectively fill two vesicle pools in frog motor nerve terminals. Neuron 27, 551–559.

Rosenmund, C., Clements, J.D., Westbrook, G.L., 1993. Nonuniform probability of glutamate release at a hippocampal synapse. Science 262, 754–757.

Rosenmund, C., Stevens, C.F., 1996. Definition of the readily releasable pool of vesicles at hippocampal synapses. Neuron 16, 1197–1207.

Ryan, T.A., 1996. Endocytosis at nerve terminals: timing is everything. Neuron 17, 1035–1037.

Ryan, T.A., Reuter, H., Smith, S.J., 1997. Optical detection of a quantal presynaptic membrane turnover. Nature 388, 478–482.

Ryan, T.A., Reuter, H., Wendland, B., Schweizer, F.E., Tsien, R.W., Smith, S.J., 1993. The kinetics of synaptic vesicle recycling measured at single presynaptic boutons. Neuron 11, 713–724.

Ryan, T.A., Smith, S.J., Reuter, H., 1996. The timing of synaptic vesicle endocytosis. Proc. Natl. Acad. Sci. USA 93, 5567–5571.

Sara, Y., Mozhayeva, M.G., Liu, X., Kavalali, E.T., 2002. Fast vesicle recycling supports neurotransmission during sustained stimulation at hippocampal synapses. J. Neurosci. 22, 1608–1617.

Schikorski, T., Stevens, C.F., 1997. Quantitative ultrastructural analysis of hippocampal excitatory synapses. J. Neurosci. 17, 5858–5867.

Schikorski, T., Stevens, C.F., 2001. Morphological correlates of functionally defined synaptic vesicle populations. Nat. Neurosci. 4, 391–395.

Schneggenburger, R., Meyer, A.C., Neher, E., 1999. Released fraction and total size of a pool of immediately available transmitter quanta at a calyx synapse. Neuron 23, 399–409.

Schote, U., Seelig, J., 1998. Interaction of the neuronal marker dye FM1-43 with lipid membranes. Thermodynamics and lipid ordering. Biochim. Biophys. Acta 1415, 135–146.

Stevens, C.F., Tsujimoto, T., 1995. Estimates for the pool size of releasable quanta at a single central synapse and for the time required to refill the pool. Proc. Natl. Acad. Sci. USA 92, 846–849.

Stevens, C.F., Wesseling, J.F., 1999. Identification of a novel process limiting the rate of synaptic vesicle cycling at hippocampal synapses. Neuron 24, 1017–1028.

Stevens, C.F., Williams, J.H., 2000. "Kiss and run" exocytosis at hippocampal synapses. Proc. Natl. Acad. Sci. USA 97, 12828–12833.

Sudhof, T.C., 1995. The synaptic vesicle cycle: a cascade of protein–protein interactions. Nature 375, 645–653.

Sudhof, T.C., 2000. The synaptic vesicle cycle revisited. Neuron 28, 317–320.

Sun, J.Y., Wu, X.S., Wu, L.G., 2002. Single and multiple vesicle fusion induce different rates of endocytosis at a central synapse. Nature 417, 555–559.

Takei, K., Mundigl, O., Daniell, L., De Camilli, P., 1996. The synaptic vesicle cycle: a single vesicle budding step involving clathrin and dynamin. J. Cell Biol. 133, 1237–1250.

Zenisek, D., Steyer, J.A., Almers, W., 2000. Transport, capture and

exocytosis of single synaptic vesicles at active zones. Nature 406, 849–854.

Zenisek, D., Steyer, J.A., Feldman, M.E., Almers, W., 2002. A membrane marker leaves synaptic vesicles in milliseconds after exocytosis in retinal bipolar cells. Neuron 35, 1085–1097.

Zhou, Q., Petersen, C.C., Nicoll, R.A., 2000. Effects of reduced vesicular filling on synaptic transmission in rat hippocampal neurones. J. Physiol. 525, 195–206 Pt 1.